J Therm Spray Tech (2021) 30:1001–1014
https://doi.org/10.1007/s11666-021-01174-2

PEER REVIEWED

Investigations on Particle Behavior at the Stagnation Zone for a Suspension Particle Jet in Plasma Spray Conditions

Alice Dolmaire[1] · Simon Goutier[1] · Michel Vardelle[1] · Pierre-Marie Geffroy[1] · Aurélien Joulia[2]

Submitted: 10 November 2020 / in revised form: 23 December 2020 / Accepted: 11 January 2021 / Published online: 7 March 2021

Abstract The suspension plasma spray process is now emerging at the industrial scale, and open questions remain regarding the formation of coatings through this process, especially regarding the relationship among particle impact, spreading and build-up into columns. Furthermore, concerns have been raised regarding the behavior of the suspension droplets in the plasma jet stagnation zone since it is a zone where plasma jet streamline directions and velocities are highly disrupted when the plasma jet impinges on a solid surface. In this study, the particle-laden jet streamlines were experimentally observed very closely to a flat surface using a particle image velocimetry technique. Submicron particles were collected in flight to determine which particles contributed to coating growth. The particle mean impact velocity against the surface was determined through image velocimetry and splat dimensions. The impact angles of the particles were also determined, and a correlation was identified with the growth angles of the columnar coating.

Keywords coating growth · columnar coating · particle velocity · particle image velocimetry · suspension plasma spraying · splat · thermal barrier coating

✉ Alice Dolmaire
alice.dolmaire@unilim.fr

[1] University of Limoges-IRCER, Limoges, France

[2] Safran Tech, Magny-les-Hameaux, France

Introduction

Suspension plasma spraying (SPS) is a process that produces a wide variety of coating microstructures. Similar to the EB-PVD (electron beam-physical vapor deposition) technique, which enables the elaboration of columnar coatings that result from the accumulation of atoms, the SPS process can produce columnar coatings from the accumulation of submicron particles. This microstructure is advantageous in thermal barrier coating applications due to its satisfactory thermomechanical resistance. The formation of these columns remains an important research focus. Various microstructures (dense, porous, feathery and cracked) can be obtained depending on the process parameters (Ref 1-8). A mapping of the plasma net power versus the total gas flow rate has revealed (Ref 5) that many coating microstructures correspond to various regimes of plasma torches. Coatings that are associated with columnar microstructures present properties such as superior thermal shock performance (Ref 6), low thermal conductivity (Ref 3, 7) or a low stress state (Ref 5). The substrate material and roughness can also influence the microstructure (Ref 1, 3, 8). Therefore, the SPS process is complex (Ref 9) and requires substantial investigation of measurements and modeling for improved understanding (Ref 10).

The other current difficulties concern the effects of the presence of the substrate, normal to the jet axis, on submicron particles' behavior and plasma flow characteristics. Experimentally, very few studies have been published in the literature regarding the influence of a substrate in front of a plasma jet on flow characteristics. Using a Rayleigh diffusion technique, Lapierre et al. (Ref 11) measured, in the presence of a cold substrate, increases in the flow temperature of 10% at 5 mm and 2.5% at 15 mm upstream of the substrate on the nozzle centerline. These results are important for the thermal treatment of nanometer-sized particles and are linked to their

time of flight and, thus, their velocities. To the best of our knowledge, no experimental study of plasma flow characteristics has been conducted similarly to the temperature measurements, namely, in the case of a flow that is blocked by a wall. It is well established that submicron particles consistently follow the flow streamlines, especially for light materials such as alumina and, to a lesser extent, zirconia. In SPS, once the suspension solvent has evaporated, the free elementary particles are melted and accelerated within the plasma jet until they reach the flow velocity, while their direction evolves according to jet fluctuations (Ref 12). If a substrate intercepts the flow, the jet streamlines deviate, and the jet mean velocity tends to zero in an area near the jet central axis (stagnation point of the flow). For particles with median diameters that exceed 10 µm, the particle inertia is sufficiently high for them to easily pass through this disrupted area upstream of the substrate without decelerating or deviating. This is not the case for very small particles, for which the competition between drag forces and inertial forces is highly sensitive (Ref 7). The additional difficulty is that in thermal spray, most particles are located in the jet center according to a Gaussian shape (Ref 13). Therefore, theoretically, in SPS, a large proportion of the submicron particles impinge the substrate with no velocity. In this theoretical scenario, very few particles would reach the substrate, stacking and flattening would be scarce, the efficiency would be very low and coatings could not be built.

Our first experimental study (Ref 14) showed that the shape and tilt of the substrate influence the submicron particle velocity, direction and coating growth in SPS. In this paper, we will characterize the kinetic behavior of submicron particles very near a flat substrate to measure their impacting velocities and incidence angles using particle image velocimetry (PIV). In-flight particle collection and SEM analysis of splats and of initial coating layers will also be conducted. These characterizations should enable us to answer the following questions:

- *What is the approximate size of the stagnation area where the plasma flow starts to deviate?*
- *Why is the coating always thicker and denser in the center of the particle jet, which is a zone where particles have theoretical velocities that are near zero?*
- *Which particles contribute to the growth of columns in SPS and how?*

Experimental Methods and Details

Spraying Conditions and Experiments

A cascaded arc plasma torch, namely a TriplexPro-210 from Oerlikon-Metco (Kelsterbach, Germany), was used to spray the suspension and produce the studied coatings. A 6.5-mm nozzle (diameter) was mounted on the torch.

The suspension was produced with an 8 mol.% yttria-stabilized zirconia (YSZ) commercial powder of mean particle size $D_{50} = 0.54$ µm from IMERYS Fused Minerals (Laufenburg, Germany) and a dispersing agent (Cerampilot, Limoges, France). These materials were mixed together for a particle loading of 5 wt.% in ethanol. Then, the suspension was subjected to constant agitation to avoid any sedimentation prior to spraying. The injection system was radial to the plasma jet (diameter 150 µm). The suspension flow rate was approximately 35 mL min^{-1}.

The substrates that were used for the study were placed at a standoff distance of 60 mm. They were composed of water-cooled rectangular stainless steel plates with dimensions of 3 × 1.5 × 1.5 cm^3. During the PIV measurements, the stainless steel plates were immobilized. These details are summarized in Fig. 1.

Next, cross sections of the microstructures of the initial layers that were deposited on the stainless steel rectangular plates in this configuration were observed using a JEOL IT300 LV (Jeol Europe, Croissy sur Seine, France) scanning electron microscope (SEM). Similarly, splats were collected on mirror-polished stainless steel buttons with a diameter of 25 mm, and their surfaces were observed with the same SEM.

Particle Image Velocimetry Principle and Setup

Particle image velocimetry consists in measuring movements of small particles that are dragged in a fluid using an advanced optical setup in combination with a digital image correlation technique. The system is illustrated in Fig. 2. It is composed of two high-speed cameras (1 µs of exposure time) that are positioned orthogonally to each other and collect the same converging light from a beam splitter. A macrolens is attached to the first camera and determines the size of the region of interest (ROI) that is examined. In this study, the ROI had dimensions of 1.5 × 1 × 1 mm^3. A

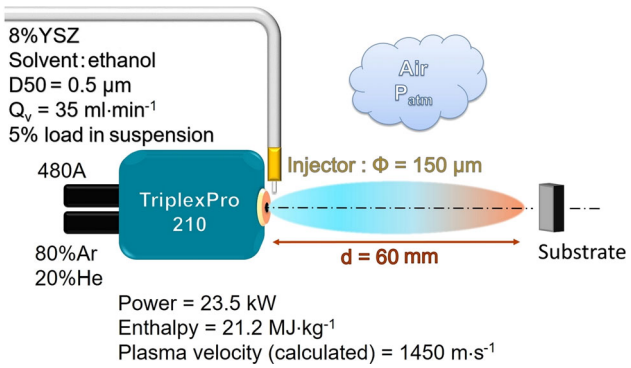

Fig. 1 Diagram of the spraying settings and conditions

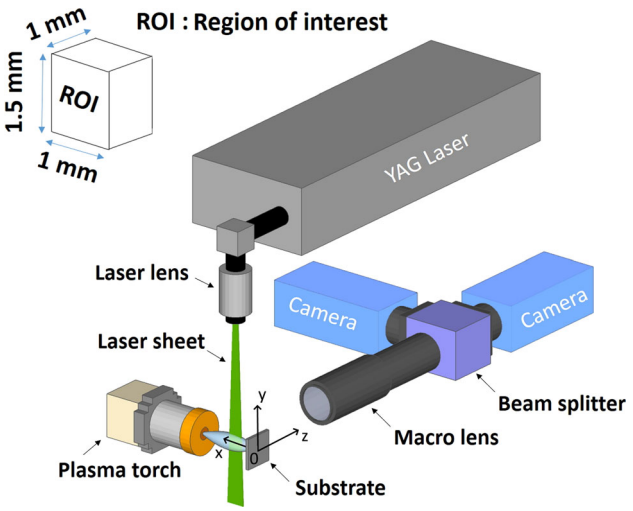

Fig. 2 Diagram of the PIV setup

double-pulsed Nd-YAG laser (wavelength $\lambda = 532$ nm) was used to seed particles into a flow in the field. The two cameras were separately synchronized to a single laser pulse at a time to detect a movement in each pair of frames. The time gap between the pulses was set at 0.12 µs.

For this study, from 100 to 200 frames were captured within the plasma jet at various positions from the substrate or along the substrate surface. From these frames, Eulerian velocity fields were calculated using the software DaVis 8 (LaVision, Göttingen, Germany). Then, the average magnitudes of the velocity vectors and their angles were extracted for each spatial position within the ROI. An average measurement error of 20 m s^{-1} on particle velocity and of 2.5° on the velocity angle were estimated from the slight variations of the substrate position between identical experiments.

Particle Collection and Flattening of Splats

A particle collector was used to determine particle sizes after a heat treatment using plasma (Fig. 3). Particles were collected in flight at the tip of the plasma jet. However, various technical issues were encountered in the collection of in-flight submicron particles. First, they possess a small momentum; hence, they cannot be captured with a conventional collector. Second, these particles can be easily sucked away by air aspiration and, thus, lost to collection.

To resolve these issues, the collector was homemade and consisted of several parts: A water-cooled stainless steel pipe was built and linked to a water tank. The bottom of the pipe was dipped into water, in which particles would become trapped. To force this particle entrapment, a slight underpressure was continuously maintained in the tank. In addition, an anti-splashing system was implemented to suppress the loss of fine particles onto the walls of the tank. An exhaust was also used to extract the plasma gases that passed through the pipe and tank.

Once the collection was complete, the liquid in the collector was retrieved and allowed to sediment, and the sediment was dried. After dilution in ethanol, the particle size distributions of this new suspension, which contained the collected particles, were measured using a laser diffractometer (LA-960, HORIBA Ltd, Japan).

To evaluate the performance of this particle collector, various experiments were conducted. These quality experiments were conducted without plasma on powder that was dispersed by compressed air. Three types of powder sizes were selected. After passing through the collection device, the collected particles were analyzed using a laser diffractometer. The results demonstrated that the particle size distribution of the collected powder was identical to that of the incidental powder in each case (Table 1).

The slight decrease in D_{50} after collection (less than 2.5% for the smallest particles) was judged as reasonable. Therefore, the use of this homemade system to analyze the reduction or increase in the median diameter of in-flight submicron particles within a plasma jet was approved.

The median diameter of the particles that impact the substrate being known, a careful analysis of the resulting splat diameters enabled us to accurately estimate flattening ratios. It is possible to calculate an impact velocity for impinging particles from the center of the jet via various inverse methods using the flattening ratio (Ref 15, 16). However, these laws were established for particles with a median size that exceeds 10 µm. The only study that considers the impact conditions for submicron particles is that of Bidron et al. (Ref 17). The impact velocity equation that was obtained by Bidron (adaptation of the equation of Bertagnolli (Ref 16) to the submicron particles that are used in SPS) is as follows:

$$\xi = 0.890 * R_e^{0.2} \quad \text{(Eq 1)}$$

where ξ is the flattening ratio and Re is the Reynolds number.

From this equation, it is possible to deduce the particle impact velocity v_{impact} from the Reynolds number:

$$v_{\text{impact}} = \frac{\eta D^4}{\rho}\left(\frac{1}{0.890 * d}\right)^5 \quad \text{(Eq 2)}$$

where η and ρ represent the dynamic viscosity and the density, respectively, of the liquid material; D is the mean splat diameter; and d is the mean diameter of the collected particles.

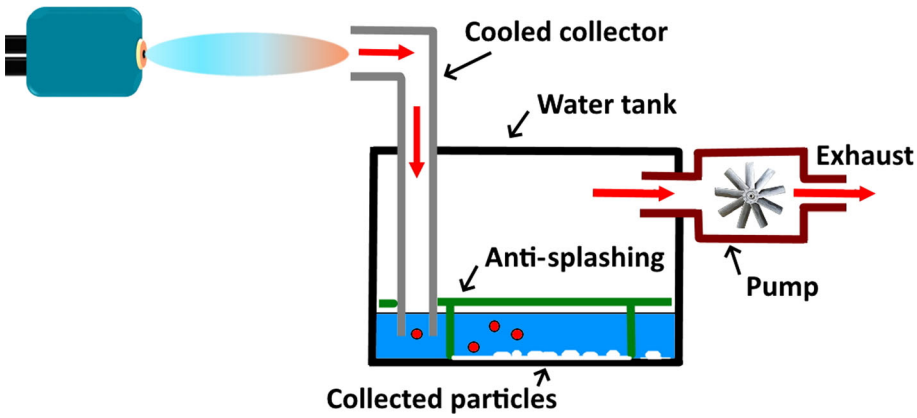

Fig. 3 Particle collector

Table 1 Median particle sizes D50 and standard deviation σ before and after collection

Experiment	Before collection	After collection
1	D_{50} = 0.54; σ = 0.21	D_{50} = 0.52; σ = 0.2
2	D_{50} = 5.87; σ = 2.34	D_{50} = 5.73; σ = 2.08
3	D_{50} = 30.79; σ = 8.71	D_{50} = 29.15; σ = 7.53

Results and discussion

The objective of this study is to characterize the behavior of submicron particles that are trapped in a plasma jet that is impinging a substrate surface. The jet area that is targeted in this study is the stagnation zone, which is defined as the zone where the substrate's presence disturbs the particle velocity. To investigate this zone, a tiny PIV field of analysis was selected (approximately 1.5 × 1 × 1 mm^3) to examine particle streamlines within areas that were nearest to the substrate surface.

Thus, the study was conducted as follows:

- Axially in a range from x = 100 µm to 20 mm from the substrate surface;
- Radially from the central plasma jet streamlines at y = 0, 5 and 10 mm from the surface.

The objective is to measure the decrease in the particle velocity and the variation in particle direction within various areas of the plasma jet, especially the stagnation zone.

Axial evolution of the particle velocity at the center of the plasma jet upstream of the substrate

To examine the influence of the stagnation zone on the in-flight particle velocities, measurements were taken in the presence and absence (free jet case) of the substrate. The results of these tests are presented in Fig. 4.

Each point of the graph represents the magnitude of the particle velocity averaged over 100 frames on the plasma jet axis. First, submicron particle velocities decrease naturally in a free plasma jet over the last ten millimeters; however, values remain at approximately 400 m s^{-1} on this central streamline. Second, due to the substrate presence at x = 0 mm (which corresponds to a distance of 60 mm from the nozzle exit), the particle velocities start to drastically decrease 5 mm before impact. The velocity decrease that is induced by the substrate is almost 300 m s^{-1} in the central area of the jet. The velocity gap between the two particle jets with and without the substrate widens until the substrate surface is reached.

As submicron particles have very little inertia, their behavior is directly influenced by any abrupt changes in the plasma jet. The impressive drop of velocities in the jet center in a few millimeters is due to the formation of a stagnation zone of the plasma flow. In fluid dynamics, a stagnation zone is the area where the axial component of the jet velocity decreases abruptly and the radial component slightly increases. In the presence of an obstacle, this deceleration leads to an increasing static pressure of the fluid at the stagnation point. Moreover, particle or drop movements in a fluid depend on their time response in relation to the flow time scale. This can be evaluated through the Stokes number ($\mathrm{St} = \frac{1}{18}\frac{\rho_p d_p^2 v_g}{\mu_g D}$). Our previous study on the matter (Ref 14), which was conducted with the same suspension and plasma conditions, has shown that this number remains below 0.5 along the central axis from the nozzle exit to the tip of the plasma plume at approximately x = 60 mm. Hence, submicron particles that are trapped in the plasma jet strictly follow any variations of the flow along the x-axis. Thus, the huge drop in velocities in the last 5 millimeters before impact corresponds to a change in regime from the free plasma jet to the stagnation zone. These results are in agreement with our previously published results (Ref 14), namely, the presence of the substrate substantially affects the particle velocities and

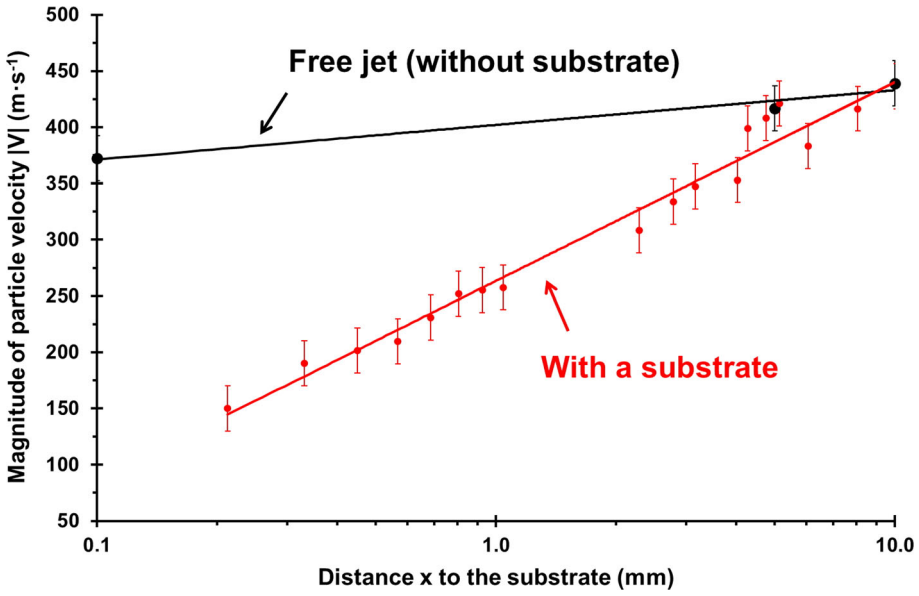

Fig. 4 Axial evolution of the particle average velocity |*V*| at the center of the plasma jet in a free jet case and in a jet that is impinging a substrate at a 60 mm stand-off distance (x = 0 mm)

PIV measurements can be used to more accurately define the plasma jet stagnation zone.

Radial Evolution of the Particle Velocity at Various Distances from the Substrate Surface

The previous results highlight the important decrease of the particle velocity at the center of a plasma jet that is impinging a substrate and provide an approximate length of the stagnation zone. *However, what occurs in areas away from the center, in the fringes of the jet? Can we specify the radius of this stagnation zone in front of a flat substrate?*

The following figures display the evolutions of the mean velocity of particle streamlines as a function of their position in relation to the plasma jet axis (Fig. 5a) and the particle orientation α in relation to the substrate surface normal for each of these positions (Fig. 5b).

Figure 5a shows the following:

- At distance x = 10 mm from the substrate, the mean velocity decreases radially very fast with a difference of approximately 350 m s^{-1} between y = 0 mm and y = 10 mm.
- The highest slowdown of particles is registered on the plasma jet axis (y = 0 mm). Velocities drop from 450 to 100 m s^{-1} in 20 mm.
- The particle velocity remains almost constant at a value of approximately 200 m s^{-1} at y = 5 mm away from the plasma jet center streamlines.
- At the periphery of the plasma jet (y = 10 mm), the particle velocity increases from 75 m s^{-1} up to a threshold value of 250 m s^{-1}, which is maintained in the last 500 µm before impact.

Approximately x = 1 mm from the substrate surface, the velocity values from the central and peripheral streamlines are approximately equal, with all detected particles traveling at a velocity of approximately 200 m s^{-1}. Below 1 mm, velocities at the center of the plasma jet continue to decrease and become lower than the particle velocity at the periphery approximately 400 µm before impact. Thus, the substrate and, therefore, the stagnation zone affects the submicron particle velocity evolution both at the center of the plasma jet and on its far outskirt. The substrate negatively affects particle velocity values at the center of the plasma jet due to flow braking, while particles that are trapped at the periphery of the plasma jet are accelerating when they encounter the spread of the jet at the substrate surface.

This last hypothesis is supported by the analysis of the average angle α (the error on each angle is approximately 2.5°) of the particle velocity vectors as a function of their position within the plasma plume (Fig. 5b). Indeed, up to 10 mm before the substrate, the particle deviation corresponds to the natural aperture of the plasma jet without any substrate, namely, an opening angle of 2° at y = 0 mm, 10° at y = 5 mm and 20° at y = 10 mm. From x = 10 mm going downstream to the substrate surface, particles start to strongly deviate until impact, with registered angles that evolve from 10° to 55° at y = 5 mm at the center of the plasma jet and from 20° to up to 80° at the periphery of the plasma jet (y = 10 mm). Thus, particles at the periphery of the plasma jet encounter a wall jet that is parallel to the substrate surface and are accelerated within the flow. The particles within the plasma jet central streamlines barely deviate along their way to impact, as the particle velocity angles remain at

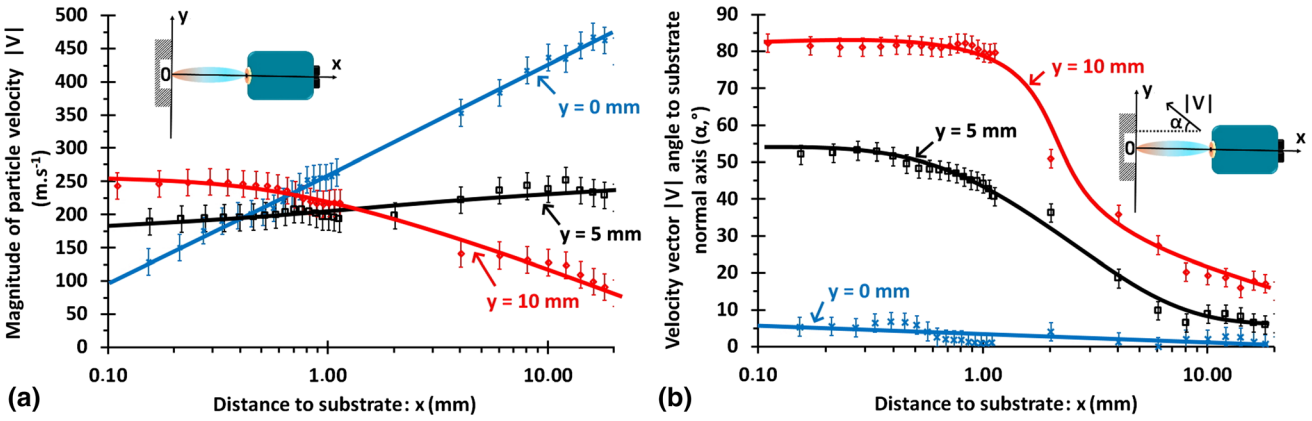

Fig. 5 Evolutions of (a) the average magnitude of the particle velocity and (b) the velocity vector angle with the radial position from plasma jet center (y = 0 mm) and from 100 µm to 20 mm upstream from the substrate surface

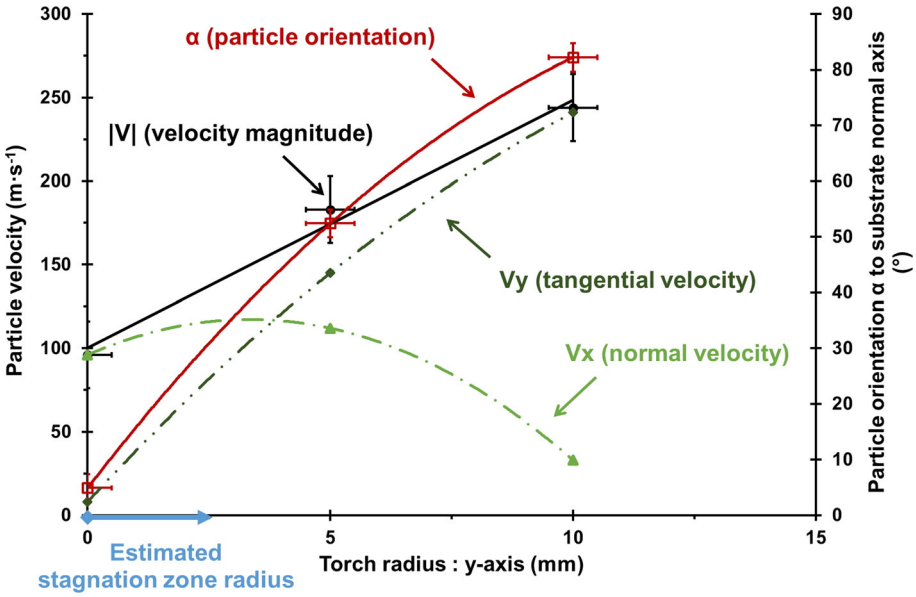

Fig. 6 Radial evolution of the velocities in a jet section 100 µm upstream of the substrate and of the particle orientation α from the torch axis

approximately 5°, namely, the plasma jet streamlines are almost perpendicular to the substrate surface.

Therefore, the velocity magnitude is increasing very fast along the y-axis with a velocity minimum in the center (Fig. 6), and the corresponding radius of the stagnation zone can be estimated to be equal to a few millimeters, namely, below 5.

As shown in Fig. 6, the normal components of the particle velocity remain broadly constant until 6 mm in radius, at approximately 100 m s^{-1}. This value would be beneficial for the flattening of droplets and the formation of splats. The next paragraph addresses a study of splats that result from droplet impacts from both the stagnation zone and the plasma jet periphery.

Flattening of droplets and the impact velocity of particles

In this next section, the following questions are considered: *Are all the particles impacting the substrate and forming splats? Are the low impact velocities registered by PIV realistic?*

As discussed previously, the impact velocity can be estimated via in-flight particle collection in association with an analysis of splat flattening. The results of the particle median sizes before and after plasma heat treatment are presented in Table 2.

According to the analysis of the particle size distributions before and after thermal spraying, no change is detected in the median size when only the number data are considered. However, according to the volume calculation,

Table 2 Comparison of the particle median sizes (number and volume) in the suspension before and after treatment by plasma

D_{50} (number averaged)		D_{50} (volume averaged)	
Initial powder	After plasma treatment	Initial powder	After plasma treatment
0.07 µm	0.07 µm	0.54 µm	0.71 µm

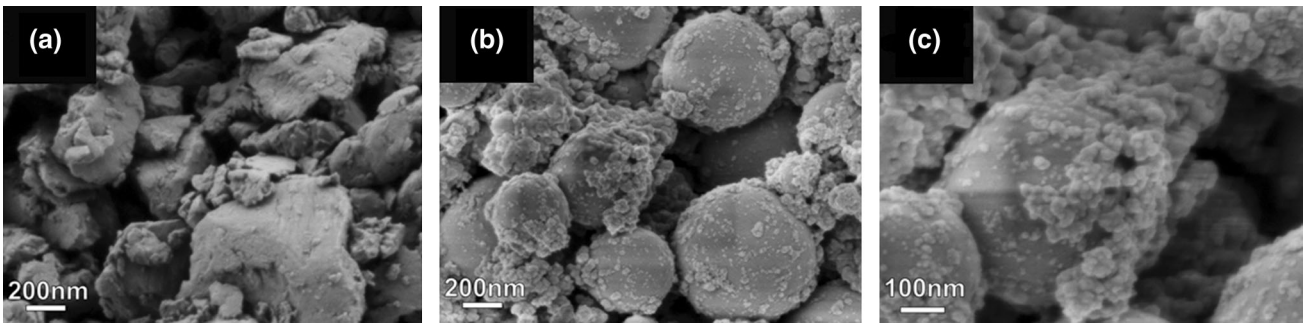

Fig. 7 SEM images of particles from the commercial powder (a) and particles that were collected in-flight (b, c magnification × 2)

the median size increases after treatment by the plasma jet from 0.54 µm to 0.71 µm. Hence, the occurrence of in-flight particle agglomeration is posited, which would increase the average particle diameter by almost 31% in this case. Observations via SEM were conducted to evaluate this assumption (Fig. 7).

The SEM images of the particles before and after plasma spraying enable the establishment of assumptions on the in-flight behavior of the suspension particles: Before the plasma heat treatment, the suspension particles are angular and disk-shaped. Once collected after their heat treatment by the plasma jet, the particles are spherical in a wide range of diameters, with larger particles melting and agglomerating. It is observed at the highest magnification (Fig 7c) that the smallest particles are composed of very fine particles, which are also melted. These particles, which are characterized by their grape-like appearance, are further indications of the occurrence of an agglomeration process during flight.

Then, splats were collected at a distance of 60 mm from the torch nozzle exit on flat and mirror polished surfaces. To obtain these splats, the torch was moved laterally at a speed of 1 m s^{-1}. Substrates were tilted with an increasing angle in front of the plasma jet on a lateral path; hence, the yttria zirconia particles that evolved mainly in the jet center impacted with an increasing angle of incidence. This setup of titled substrates enables the segregation of impacts from particles that gradually move from the center to the periphery of the plasma jet. The assembly is illustrated in Fig. 8.

The resulting micrographs (Fig. 9) show that the splat concentration on the substrate surface decreases when the incidence angle of the molten particles with the normal of the substrate increases. These SEM observations underline that submicron particles follow the direction and the general orientation of the plasma jet, as observed previously by PIV. The increasing incidence of the particle flow also induces a reduction of the velocity normal components (Fig. 6). This leads to decreasing contributions from the particles to the formation of the first splats (decreasing concentration of splats) and, therefore, of the first deposition layers. These results are in agreement with observations of Kang et al. (Ref 18) for 40 µm particles that were impacting tilted surfaces.

These micrographs also show the influence of the molten particle angle on the splat flattening and shape. As the impact angle of incidence increases, the splats become increasingly elongated ellipses (see Fig. 9 from 0° to 70°). The major and minor diameters of these ellipses were measured by ImageJ, which enabled the acquisition of the number distributions of the sizes of the splats according to the angle of incidence of the impacting particles. The evolutions of the major and minor median diameters as functions of the impacting angle of incidence are presented in Fig. 10.

The major median diameter increases sharply with increasing impacting angle. Its value doubles between 0° and 70°. This corresponds to the preferential flattening of the particles in the direction of the impact. The minor diameter decreases as the impact angle increases and may be related to the initial median diameter of the drops on

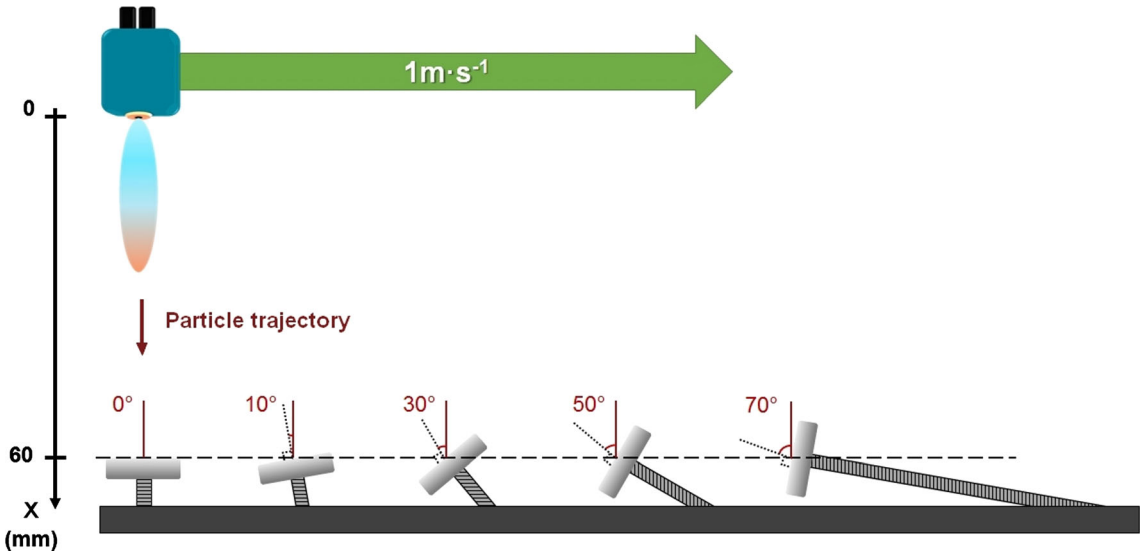

Fig. 8 Setup for obtaining splats at various incidence angles

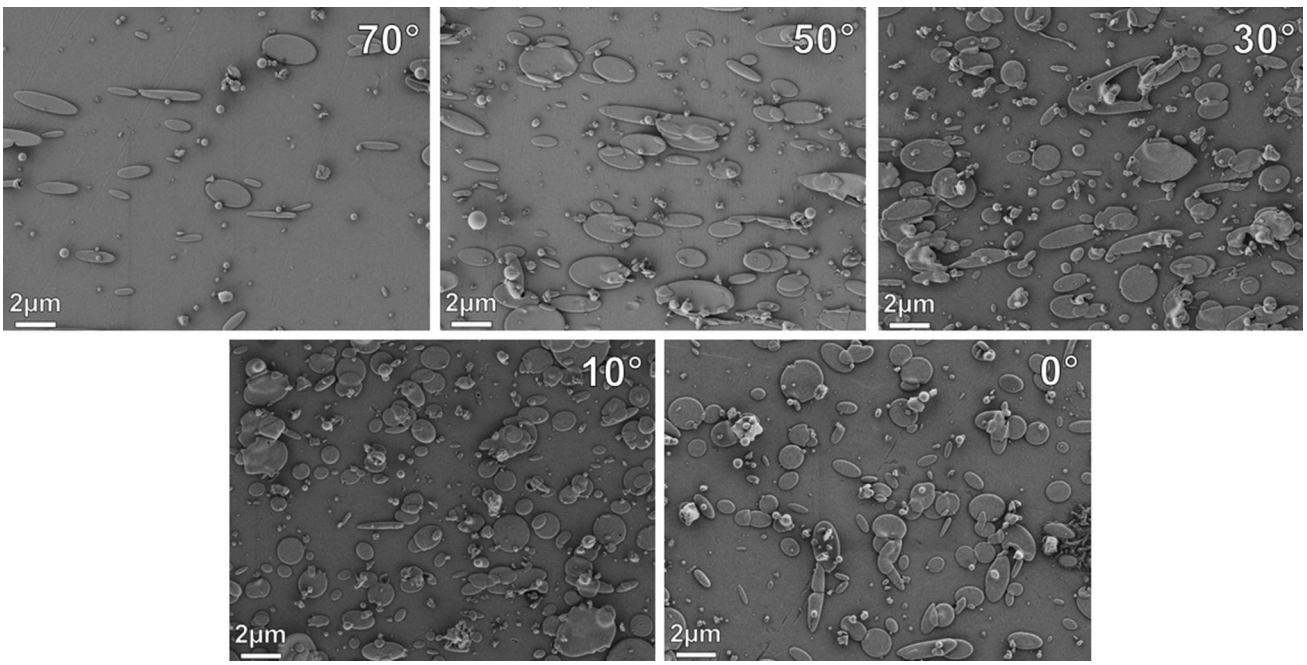

Fig. 9 Splats that were obtained at various incidence angles (between the plasma jet axis and the normal of the substrate) of the melted YSZ submicron particles

impact. Measurements at 70°, where the splats are most distorted along the axis of the inclination, indicate that most of the particles that form splats have a median diameter of 0.7 µm. An equivalent median circular diameter was also calculated. The circular median diameter of the splats changes minimally as a function of the inclination, namely, from a median diameter of 1.1 µm at 0° to 1.2 µm at 70°.

On the examined surfaces (Fig. 9), the present entities (melted or unmelted) have diameters that exceed 0.3 µm. The particles with diameters of less than 0.3 µm do not seem to be able to adhere to the substrate, whereas the in-flight particle collection has demonstrated their presence in the plasma jet (Table 2). Near the impact surface, a 0.3-µm particle has a Stokes number of approximately 0.01, which is substantially less than the critical value of approximately 0.2 according to the calculations of Mauer (Ref 19) ; hence, the 0.3-µm particle follows the streamlines of the flow without sticking to the substrate. A volume analysis of the particle size distribution of the particles that were collected

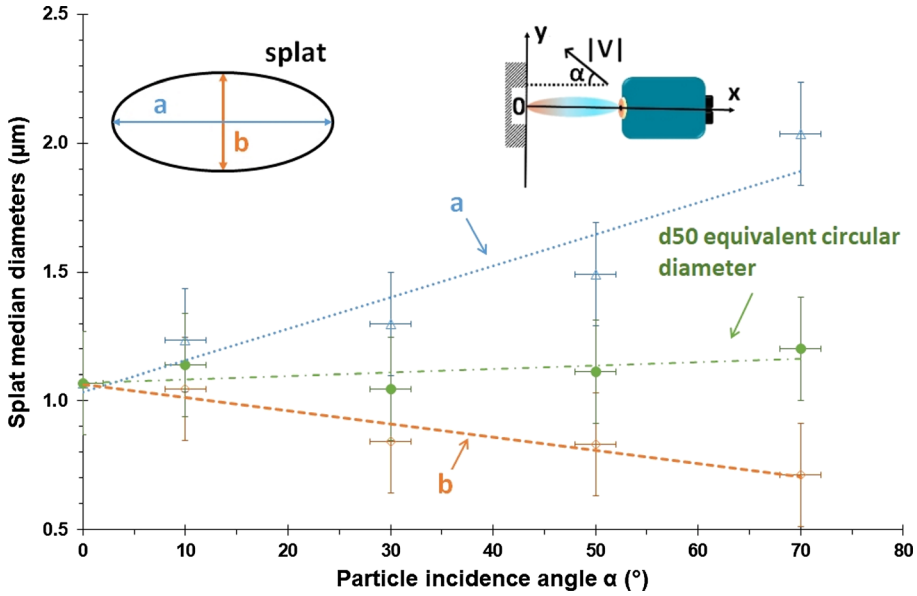

Fig. 10 Splat diameters versus particle incidence angles

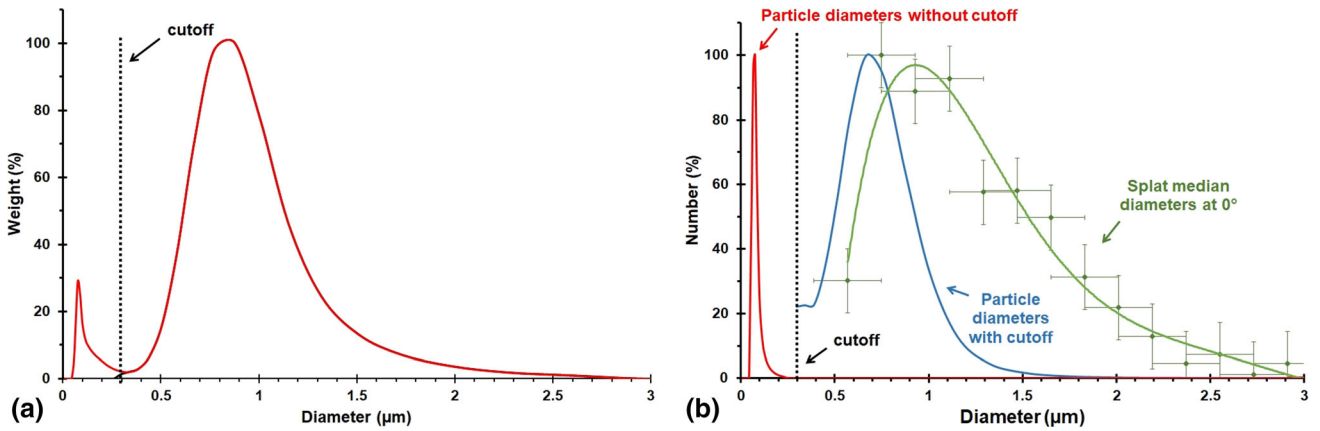

Fig. 11 (a) Measured particle size distribution in weight after collection and (b) particle and splat size distributions at 0° in number with and without the cutoff

"in flight," which is presented Fig. 11(a), shows that this majority of very fine particles (< 0.3 µm) represents 30% of the total mass. As these fine particles do not contribute to the formation of the first splats and adhere very little to the substrate surface, it is necessary to identify the median profile of the incident particles that impact the surface and contribute to splat flattening. As the flattening diameters of the splats are measured by image analysis and, therefore, on multiple splats, it is more relevant to focus on the number distribution of the collected particles. Thus, it is necessary to recalculate this particle size distribution from the volume distribution by applying a threshold to eliminate the values below 0.3 µm and to recalculate the number distribution [cutoff in Fig. 11(a)]. This leads to the size distribution in Fig. 11(b). Hence, once this cutoff is applied, the median size of the number distribution increases from 0.07 µm to approximately 0.67 µm.

A comparison with the median diameter of the measured splats yields a flattening ratio of 1.6 (see the case at 0° in Fig. 9). By using the relation in Eq 2 between the flattening ratio and the impact velocity of the particles, an impact velocity of approximately 170 m s^{-1} is obtained for particles that impact from the jet center. The error in this calculation is estimated to be approximately 30 m s^{-1}.

This velocity, which was determined via the analysis of splats and of the "in flight" granulometry, does not differ substantially from the value that was obtained with PIV measurements, which was approximately 100 m s^{-1} at 100 µm from the substrate surface.

In conclusion, only particles with a diameter that exceeds 0.3 µm contribute to splat formation. Moreover,

beyond an incidence angle of 30°, the normal particle velocity (< 100 m s^{-1}) is too low for many particles and fewer of them flatten onto the surface.

Column Growth

As shown in the previous sections, the particle velocity and the particle angle at impact strongly affect the splat shape (dimensions and symmetry). *What are the consequences of this influence on the coating growth and its microstructure?*

Spraying experiments without moving the plasma torch were conducted on fixed flat and sand-blasted stainless steel substrates at a standoff distance of 60 mm for 5 s to study the coating growth and characterize the influences of the particle velocity and angle on the microstructure according to the position within the plasma jet.

First, the following observations are made:

- The thickness of the deposit decreases gradually when one moves away from the plasma jet center to the periphery, which is similar to the result of Ganvir et al. (Ref 20).
- The thicknesses are similar for two radial positions that are diametrically opposed within the plasma jet, for example, $y = -5$ mm and 5 mm from the plasma jet center.
- The porosity increases in the deposit while moving away from the plasma jet center.
- Oriented columns of the deposit form along the radius of the plasma jet that is impinging the surface, with the plasma jet center as a symmetry axis.

Is there a correlation between the columnar angle β and the impact angle α of the particles? Angles β were plotted versus angles α in Fig. 12 to answer this question. Similar characterizations were recently conducted within the field of PVD thin layers (Ref 21-23) and in PS-PVD (Ref 24). Several empirical laws have been defined and evaluated over the years, thereby leading to the following general correlation between the vapor phase impact angle α and the column growth angle β:

$$\tan\alpha = A\ \tan\beta \qquad \text{(Eq 3)}$$

where A is a constant that depends on the conditions of spraying, which is sometimes equal to ½.

In Fig. 12, a proportionality relation between the two angles is identified. The angle of columnar growth is always smaller than the impact angle of the particles. For this study (bold red crosses), a fitting of the results yields a value of the columnar growth angle by SPS of approximately half the value of the particle impact angle, such as $\beta = 0.42\ \alpha$. However, the relations between tan α and tan β are not constant with increasing impact angle in SPS, with values of A evolving from 0.14 to 1.73.

When comparing the various processes, the angles of columns that are obtained in the deposits are approximately identical for an impact angle value under 50°, whether in the vapor phase at an atomistic scale or with nanometer-sized particles as in the case of the study. Comparisons with the modeling results of Wang et al. (Ref 24) in PS-PVD raise questions regarding column growth. They explain that to obtain $\beta = ½\ \alpha$ with this spraying process, it is necessary for the standard deviation of the impact angle to be almost 60°. This scenario is obtained when many particles impact with a wide variety of angles around an average orientation. *Does this occur in our study?*

According to the analysis of PIV images, the vast majority of the particles retain the same angle for a

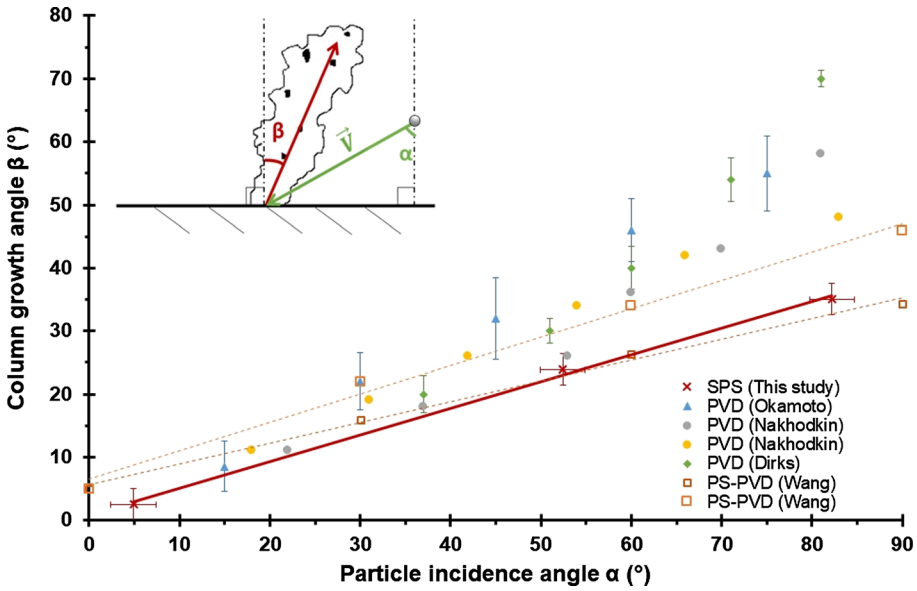

Fig. 12 Comparison between the angle β of column growth and the particle incidence angle α on the substrate (the study results are represented by red crosses and the bolded red line, other data is from (Ref 21-24)) (Color figure online)

singular spatial position within the plasma jet until approximately 100 µm away from the substrate surface. However, below 100 µm, it is assumed that these particles enter the boundary layer of the substrate surface. It is possible that these impinging particles encounter other particles that are oriented in a wall jet trajectory (plasma streamlines that are parallel to the substrate surface), namely, particles that have not impacted the surface. These wall-jet particles could participate in the thickening of the columns that are built primarily from the impinging oriented particles (low α angles). This contribution would also involve an increase in the standard deviation of the angles of local impacts on the substrate and, thus, induce the phenomenon that is proposed by the PS-PVD model, which is not possible to observe via PIV techniques.

As presented previously in Fig. 13, the total porosity of the deposit also increases when one moves away from the plasma jet center. This is a direct consequence of the impact pressure P_i of splats, as computed by G. Bidron in his PhD thesis (Ref 25) by the following formula:

$$P_i = \frac{1}{2}\rho v_x^2 \quad \text{(Eq 4)}$$

ρ represents the particle liquid density and v_x the particle normal velocity upon impact.

His calculation showed the existence of various pressure thresholds below which or above which the quality of the flattening of splats differ. Precisely, 0.7-µm yttria-stabilized zirconia particles that impact at a velocity of above 150 m s^{-1} exhibit a pressure impact that exceeds 50–60 MPa on the substrate. This pressure is sufficient for the resulting splats to mold surface roughnesses and eliminate the porosity via viscous dissipation. For an impact velocity of less than 50 m s^{-1}, which corresponds to an impact pressure of approximately 10 MPa, the capillarity tensions within the splat are too high. The splat is unable to fill in the various holes under it. Stack defects and high porosity occur in the deposit. In our study, the impact pressures of splats were calculated from normal particle velocities that were measured 200 µm before the substrate by PIV at $y = 0$, 5 and 10 mm and were compared to particle impact angles that were measured 200 µm before the substrate by PIV at $y = 0$, 5 and 10 mm (see Fig. 5b). We also used the value of 4700 kg m^{-3} for zirconia liquid density (Ref 26). These spatial positions correspond individually to the microstructures in the deposit in Fig. 13. A plot of the splat impact pressures versus the particle impact angle is presented in Fig. 14. It shows that particles that impinge with a very small incident angle onto the surface enable the highest pressure impact for splats (> 50 MPa), which corresponds to the scenario of particles coming from the center of the plasma jet and results in the center of the deposit in Fig. 13, where stack defects and pores are scarcest. In contrast, the splat impact pressures that were calculated from particles that impinge with the largest impact angle (Fig. 14, $\alpha > 80°$) are the lowest (< 5 MPa) and correspond to splats that are formed by particles that impinge from the periphery of the plasma jet. Thus, stack defects should be more frequent with such splats flattening onto the surface. This results in the microstructure at $y = \pm 10$ mm in the deposit in Fig. 13, where these defects correspond to columns and are of higher porosity.

Therefore, all these observations, which are correlated with the PIV measurements, indicate that the movement of the plasma torch and/or substrate during the SPS process is the primary parameter for the building of columnar coatings. These movements induce the impact of the most peripheral particles ($y > 5$ mm) on layers that are well stacked due to particles impacting from the plasma jet center. More precisely, particles that travel from the jet center build the column frame, while the particles on the periphery thicken these columns and give them their columnar shape by impacting with a large angle of

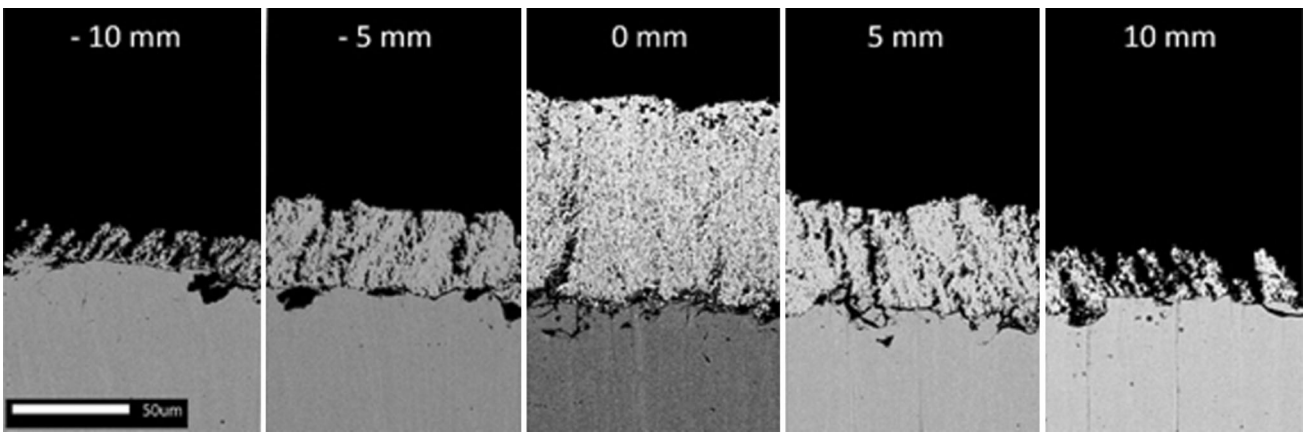

Fig. 13 SEM images of the coating at various positions from the plasma jet center streamlines ($y = 0$ mm) after 5 s of spraying onto a flat sand-blasted stainless steel substrate

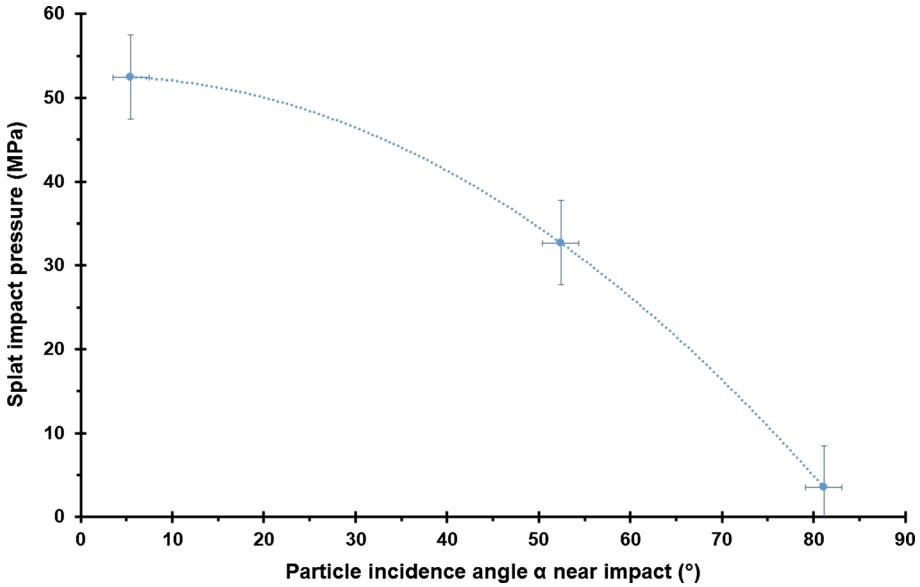

Fig. 14 Evolution of the impact pressure of splats with the particle incidence angle near impact

incidence ($\alpha > 30°$) and a low impact pressure, which triggers stack defects. These observations are in agreement with the empirical model that was developed by B. Bernard in his PhD thesis (Ref 27). Bernard's results highlight the significant effects of the torch movement on the construction and density of columns that are obtained via SPS (Ref 3, 28). These observations are also in agreement with other empirical models that show a shadowing effect of the particles in SPS in the formation of columns and the importance of surface roughness in initiating this effect (Ref 7).

Conclusions

The presence of a substrate disturbs the flow velocity field and particle trajectories in suspension plasma spraying. PIV experiments were conducted very close to the substrate, and the in-flight collection of particles that was associated with the study of particle flattening on the substrate showed the following:

- Along the torch axis, the particle velocities start to decrease drastically 5 mm upstream of the substrate surface, while in the jet periphery, the particle velocities increase.
- Approximately 1 mm before the substrate, all particles have the same velocity magnitude in a jet cross-section of 10 mm in radius but with various orientations.
- At 100 µm before the surface (PIV limitation), the particles in the jet center travel at only 100 m s^{-1}, while the particles in the periphery exhibit twice this velocity but impact the substrate with a higher incident angle (5° in the center and 80° at y = 10 mm).
- Particles at the periphery of the plasma jet (y = 10 mm) rapidly encounter a gas jet that is parallel to the substrate surface.
- Particles within the plasma jet central streamlines (below 5 mm in radius) deviate only minimally along the torch axis and are almost perpendicular to the substrate surface.
- The particle orientation directly affects the columnar growth. The columnar angles β are always approximately half the particle impact angles α, e.g., $\beta = 0.42\ \alpha$.
- Particles that evolve at the periphery of the plasma jet are the main contributors to the growth and shaping of columnar microstructures via the formation of stack defects, while column frames are primarily built by particles that impact at low angles from the center of the plasma jet.

In introduction, we asked the following questions to which this study brought some observations and conclusions:

> *What is the approximate size of the stagnation area where the plasma flow starts to be deviated?*

The limits of a stagnation zone are defined as points where the flow moving toward the substrate begins to be disturbed by the presence of a wall. Here they correspond to those of a cylinder 5mm in length and fewer millimeters in radius upstream the wall. Above this radius, the flow switches toward the periphery of the plasma jet (particle impact angle higher than 20°) and is accelerated as a "wall jet" parallel to the surface, sweeping many small particles away.

Why is the coating always thicker and denser in the center of the particle jet, a zone where particles have theoretical velocities near zero?

To conclude about the stagnation zone, a natural filtering enables the finest droplets with very small Stokes numbers to change directions (particles below 0.3 µm in diameter). Meanwhile, particles with a diameter around 1 µm exhibit an impact velocity v_x above 100 m s^{-1} and have trajectories nearly perpendicular to the substrate in this small area surrounding the center of the jet. They go through the gas boundary layer and flatten onto the substrate with enough pressure (above 50 MPa) to fill in any surface cavities. The stagnation point is also so localized in the plasma jet cross section than there are always enough particles around this point (zone where the particle Gaussian concentration is highest). In addition, particles traveling in this zone benefit from a slightly higher temperature of the flow (Ref 11) because of the presence of the substrate, and a longer time of flight thus benefit of a higher heat transfer rate. These characteristics result in the better deposition efficiency of less porous SPS coatings at the center of the particle jet, a feature which is commonly observed.

The particle mean size and size distribution are thus the main parameters to achieve a specific SPS coating microstructure.

Which particles are really contributing to the growth of columns in SPS and how?

Particles around and above 0.7 µm impinging from the center of the jet with enough velocity will contribute in making stacks of rounded splats with the least defects, i.e., the least porosity. Therefore, these particles will make up most of the columnar skeleton, perpendicular to the substrate surface. Meanwhile, micron-sized particles impinging onto the surface from an angle α above 5° will make stacks of splats with many defects and will help contribute orientating the coating growth in their direction of incidence, such as $\beta = 0.42\ \alpha$. These particles directly shape the columns in SPS in a cauliflower formation.

The smaller particles will not contribute in making splats but will get trapped during the coating formation and will correspond to the many rounded melted grains observed in SPS coating microstructures. These particles further help obtaining a multiscale porosity, typical of these coatings (Ref 28).

References

1. N. Curry, K. VanEvery, T. Snyder, J. Susnjar and S. Bjorklund, Performance Testing of Suspension Plasma Sprayed Thermal Barrier Coatings Produced with Varied Suspension Parameters, *Coatings*, 2015, **5**(3), p 338-356.
2. X. Chen, S. Kuroda, T. Ohnuki, H. Araki, M. Watanabe and Y. Sakka, Effects of Processing Parameters on the Deposition of Yttria Partially Stabilized Zirconia Coating During Suspension Plasma Spray, *J. Am. Ceram. Soc.*, 2016, **99**(11), p 3546-3555.
3. B. Bernard, L. Bianchi, A. Malié, A. Joulia and B. Rémy, Columnar Suspension Plasma Sprayed Coating Microstructural Control for Thermal Barrier Coating Application, *J. Eur. Ceram. Soc.*, 2016, **36**(4), p 1081-1089.
4. D. Zhou, O. Guillon and R. Vaßen, Development of YSZ Thermal Barrier Coatings Using Axial Suspension Plasma Spraying, *Coatings*, 2017, **7**(8), p 120-137.
5. R.C. Seshadri, G. Dwivedi, V. Viswanathan and S. Sampath, Characterizing Suspension Plasma Spray Coating Formation Dynamics through Curvature Measurements, *J. Therm. Spray Technol.*, 2016, **25**(8), p 1666-1683.
6. A. Ganvir, S. Joshi, N. Markocsan and R. Vassen, Tailoring Columnar Microstructure of Axial Suspension Plasma Sprayed TBCs for Superior Thermal Shock Performance, *Mater. Des.*, 2018, **144**, p 192-208.
7. K. VanEvery, M.J.M. Krane, R.W. Trice, H. Wang, W. Porter, M. Besser, D. Sordelet, J. Ilavsky and J. Almer, Column Formation in Suspension Plasma-Sprayed Coatings and Resultant Thermal Properties, *J. Therm. Spray Technol.*, 2011, **20**, p 817-828.
8. Y. Zhao, Z. Yu, M.-P. Planche, A. Lasalle, A. Allimant, G. Montavon and H. Liao, Influence of Substrate Properties on the Formation of Suspension Plasma Sprayed Coatings, *J. Therm. Spray Technol.*, 2018, **27**, p 73-83.
9. A. Vardelle, C. Moreau, J. Akedo, H. Ashrafizadeh, C.C. Berndt, J. Oberste Berghaus, M. Boulos, J. Brogan, A.C. Bourtsalas, A. Dolatabadi, M. Dorfman, T.J. Eden, P. Fauchais, G. Fisher, F. Gaertner, M. Gindrat, R. Henne, M. Hyland, E. Irissou, E.H. Jordan, K. Aik Khor, A. Killinger, Y.-C. Lau, C.-J. Li, L. Li, J. Longtin, N. Markocsan, P.J. Masset, J. Matejicek, G. Mauer, A. McDonald, J. Mostaghimi, S. Sampath, G. Schiller, K. Shinoda, M.F. Smith, A. Ansar Syed, N.J. Themelis, F.-L. Toma, J. Pablo Trelles, R. Vassen and P. Vuorist, The 2016 Thermal Spray Roadmap, *J. Therm. Spray Technol.*, 2016, **25**(8), p 1376-1440.
10. E. Dalir, A. Dolatabadi and J. Mostaghimi, Modeling of Suspension Plasma Spraying Process Including Arc Movement Inside the Torch, *J. Therm. Spray Technol.*, 2019, **28**, p 1105-1125.
11. D. Lapierre, R.J. Kearney, M. Vardelle, A. Vardelle and P. Fauchais, Effect of a Substrate on the Temperature Distribution in an Argon-Hydrogen Thermal Plasma Jet, *Plasma Chem. Plasma Process.*, 1994, **14**(4), p 407-423.
12. R. Etchart-Salas, V. Rat, J.-F. Coudert, P. Fauchais, N. Caron, K. Wittman and S. Alexandre, Influence of Plasma Instabilities in Ceramic Suspension Plasma Spraying, *J. Therm. Spray Technol.*, 2007, **16**(5-6), p 857-865.
13. K. Bobzin, W. Wietheger, M.A. Knoch and S.R. Dokhanchi, Estimation of Particle Mass Flow Rate in Free Jet Using In-Flight Particle Diagnostics in Plasma Spraying, *J. Therm. Spray Technol.*, 2020, **29**, p 921-931.
14. A. Dolmaire, S. Goutier, A. Joulia, P.-M. Geffroy, M. Vardelle and L. Bianchi, Experimental Study of the Impact of Substrate Shape and Tilting on Particle Velocity in Suspension Plasma Spraying, *J. Therm. Spray Technol.*, 2020, **29**, p 358-367.
15. Y. Tanaka and M. Fukumoto, Investigation of Dominating Factors on Flattening Behavior of Plasma Sprayed Ceramic Particles, *Surf. Coat. Technol.*, 1999, **120-121**, p 124-130.
16. M. Bertagnolli, M. Marchese and G. Jacucci, Modeling of Particles Impacting on a Rigid Substrate Under Plasma Spraying Conditions, *J. Therm. Spray Technol.*, 1995, **4**(1), p 41-49.
17. G. Bidron, S. Goutier, M. Vardelle, P. Denoirjean and P. Fauchais, Flattening Behavior of Micro- and Nano-Sized Yttria-

Stabilized Zirconia Particles Plasma-Sprayed on Smooth Preheated (610 K) Nickel Substrate: Part I, *J. Phys. Appl. Phys.*, 2019, **52**(16), p 165201. https://doi.org/10.1088/1361-6463/aafd81
18. C.W. Kang, H.W. Ng and S.C.M. Yu, Imaging Diagnostics Study on Obliquely Impacting Plasma-Sprayed Particles Near to the Substrate, *J. Therm. Spray Technol.*, 2006, **15**(1), p 118-130.
19. G. Mauer, Numerical Study on Particle-Gas Interaction Close to the Substrates in Thermal Spray Processes with High-Kinetic and Low-Pressure Conditions, *J. Therm. Spray Technol.*, 2019, **28**, p 27-39.
20. A. Ganvir, R.F. Calinas, N. Markocsan, N. Curry and S. Joshi, Experimental visualization of microstructure evolution during suspension plasma spraying of thermal barrier coatings, *J. Eur. Ceram. Soc.*, 2019, **39**(2-3), p 470-481.
21. K. Okamoto, T. Hashimoto, K. Hara and E. Tatsumoto, Origin of Magnetic Anisotropy of Iron Films Evaporated at Oblique Incidence, *J. Phys. Soc. Jpn.*, 1971, **31**(5), p 1374-1379.
22. N.G. Nakhodkin and A.I. Shaldervan, Effect of Vapour Incidence Angles on Profile and Properties of Condensed Films, *Thin Solid Films*, 1972, **10**(1), p 109-122.
23. A.G. Dirks and H.J. Leamy, Columnar Microstructure in Vapor-Deposited Thin Films, *Thin Solid Films*, 1977, **47**(3), p 219-233.
24. P. Wang, W. He, G. Mauer, R. Mücke and R. Vaßen, Monte Carlo simulation of column growth in plasma spray physical vapor deposition process, *Surf. Coat. Technol.*, 2018, **335**, p 188-197.
25. G. Bidron, "Etude physicochimique multi-échelle des interfaces pour la compréhension de l'adhérence d'un dépôt par projection thermique de poudres submicroniques" (Physicochemical multi-scale study of splat- substrate interfaces for adhesion understanding in suspensions plasma spraying (SPS)), Ph.D. Thesis, University of Limoges, 2014 (in French)
26. T. Kondo, H. Muta, K. Kurosakin, F. Kargl, A. Yamaji, M. Furuya and Y. Ohishi, Density and Viscosity of Liquid ZrO2 Measured by Aerodynamic Levitation Technique, *Heliyon*, 2019, **5**(7), p e02049. https://doi.org/10.1016/j.heliyon.2019.e02049
27. B. Bernard, Barrières thermiques par projection plasma de suspensions: développement et caractérisation de microstructures à faible conductivité thermique" (Thermal barrier coatings performed by suspension plasma spraying: Development and characterization of low thermal conductivity microstructures), Ph.D Thesis, Lorraine University, 2016 (in French)
28. B. Bernard, A. Quet, L. Bianchi, V. Schick, A. Joulia, A. Malié and B. Rémy, Effect of Suspension Plasma-Sprayed YSZ Columnar Microstructure and Bond Coat Surface Preparation on Thermal Barrier Coating Properties, *J. Therm. Spray Technol.*, 2017, **26**, p 1025-1037.